

COVER PAGE

Document downloaded by @DAEL

Fri Nov 27 15:06:29 2026
For personal use

When automatic English translation is provided, only the original document is authentic.
The EAA cannot be held responsible of any translation error

Bibliographical reference

A Coupled FE and DtN Mapping Method for the Exterior Problem of the Helmholtz Equation in an Oceanic Waveguide, W. F. Pan, Y. X. You, G. P. Miao and Z. Q. Li, Acta Acustica **vol. 94** (Number 2), 2008, pp. 301-309

DOI
https://doi.org/10.3813/AAA.918033

ACTA ACUSTICA UNITED WITH ACUSTICA
Vol. 94 (2008) 301 – 309
DOI 10.3813/AAA.918033

A Coupled FE and DtN Mapping Method for the Exterior Problem of the Helmholtz Equation in an Oceanic Waveguide

W. F. Pan[1,2], Y. X. You[1], G. P. Miao[1], Z. Q. Li[2]
[1)] School of Naval Architecture, Ocean and Civil Engineering, Shanghai Jiaotong University, Shanghai 200030, China
[2)] School of Science, Wuhan University of Technology, Wuhan 430070, China

Summary
The interaction of acoustic waves with a scattering object in an oceanic waveguide was considered. A finite-element method was developed to solve numerically the acoustic scattering problem based on the Galerkin variational principle and the DtN mapping method. The results show that the proposed method is valid and its numerical implementation is very fast. Moreover, the characteristics of the scattering waves by an obstacle in an oceanic waveguide and multiple scattering effects between the obstacle and the waveguide boundaries were numerically analysized.

PACS no. 43.20.Fn

1. Introduction

The study of the interaction of acoustic waves with scattering objects is important because of its considerable application in the military and civil fields. To date, there have been many methods for dealing with such scattering problems in the case of the free space, including analytic methods, Boundary Element Method (BEM), and Finite Element Method (FEM) ([1, 2, 3] and references therein). It is reasonable to reduce such acoustic scattering problems for the case where scattering objects or acoustic sources are far from both the surface and the bottom of the ocean. However, the influence of both the free surface and the bottom of the ocean on the acoustic propagation in the case of a shallow water can not be neglected. In this case, the oceanic waveguide is a more practical mathematic model. Comparing to the case of the free space, the echo structural characteristics of scattering objects will be more complex and difficulty to be numerically analysized.

The Boundary element method (BEM) is the primary method for the numerical solution of the acoustic scattering problems of objects in an oceanic waveguide [4, 5, 6, 7, 8]. Its main advantage is in the reduction of problem dimensions, but many difficulties will be faced for its numerical solution. First, its integral kernel with the singularity causes great difficulty. Second, it will not have unique solution with some wavenumbers. Although there are some approaches to avoid such drawbacks, for example, the CHIEF method and the method with modifying integral kernel. However, for the CHIEF method, the reasonable selection of “CHIEF points" is theoretically difficulty, and the method with modifying integral kernel will lead to the higher singularity and the more difficulty for its numerical solution. Third, though the BEM has the advantage of reduction of problem dimensions, the generated linear equations are full rank and its computational cost is rather great, especially for three dimensional problems. Finally, since the Green’s function in an oceanic waveguide is an infinite series or infinite integral [9], its convergence is very slow, thus its computational efficiency is rather low.

In recent years, some potential methods called modern BEM techniques in the case of the free space can work quite fast which is especially known from the so called Fast BEM, such as the fast multipole BEM techniques [10, 11, 12, 13, 14, 15], which overcome these drawbacks of the conventional BEM mentioned above. Moreover, some comparative study on the CHIEF method with another method was presented in [16]. It is noted that there has no report on such methods for numerically solving the interaction of acoustic waves with scattering objects in a shallow water waveguide.

In this paper, a coupled FE and DtN mapping method will be applied to solving such acoustic scattering problems of objects in an oceanic waveguide. The method was started in the pioneering work of Feng [17] , and a computational formulation was derived by Givoli and Keller [18] for converting boundary value problems defined over large or unbounded domains to formulations that are suitable for the domain-based computation. The method is motivatied by the artificial boundary conditions which are also called absorbing boundary conditions or Non-Reflecting Bound-

Received 7 November 2006,
accepted 26 July 2007.

© S. Hirzel Verlag · EAA

ary Conditions (NRBCs) for wave equations [19, 20]. In general, the use of the method can be summarized as follows:

1. Introduce an artificial boundaryΓ, which divides the original infinite domain in $R^m (m = 2, 3)$ into two domains: a finite computational domain Ω and an infinite residual domain $R^m \backslash \Omega$.
2. Solve the problem analytically in $R^m \backslash \Omega$, and then use the solution to find the Dirichlet-to-Neumann mapping(i.e. the DtN mapping) on the artificial boundary Γ.
3. Use the DtN mapping as a boundary condition on Γ to obtain a well-posed problem in Ω, and then solve numerically the problem in Ω by the finite-element method(i.e. FEM).

In what follows, for the sake of motivation and clarity, we will first consider the acoustic scattering problem by an impenetrable cylinder immersed in an oceanic waveguide. We will then proceed to an effective numerical method by the coupled FE and DtN mapping. Finally, we will give some numerical examples and demonstrate the validity and practicability of the proposed method.

2. Formulation of the problem

Let us refer to Figure 1. Let $R_H^2 = \{(x, z) | -\infty < x < +\infty, 0 \le z \le H\}$ be the region occupied by a homogeneous constant depth ocean with a free surface and a rigid bottom, such that the oxyplane lies in the surface and z-axis is vertical downwards, where H is the depth of the ocean. There is an impenetrable infinite long cylindrical obstacle D with the smooth boundary ∂D immersed in the shallow water waveguide R_H^2, whose axis is the y -axis and whose close cross section in $r = (x, z)$ plane. The water layer exterior to D is denoted as $D_e = R_H^2 \backslash \bar{D}$.

A time-harmonic line source parallel to the y-axis is placed in the exterior of the cylindrical obstacle D. Its operating circular frequency is ω and the $e^{-i\omega t}$ dependence of the field is dropped from now on. Assume that the incident line source is a normal modal wave, then it may be expressed as

$$u^i(x, z; x_s, z_s) = \sum_{n=1}^{N(k)} \frac{\mathrm{i}}{\pi k_n} \phi_n(z)\, \phi_n(z_s)\, \mathrm{e}^{\mathrm{i}k_n|x-x_s|}, \quad (1)$$

where $N(k) = [(\pi + 2kH)/2\pi]$ is the total number of the propagation modes ($[\cdot]$ denotes the integer part of the term), $\phi_n(z) = \sqrt{2/H}\sin(\gamma_n z)$ the vertical eigenfunction function, $\gamma_n = (2n-1)\pi/2H$ and $k_n = \sqrt{k^2 - \gamma_n^2}$ are the vertical and horizontal wavenumbers of the nth mode respectively, where $k = \omega/c_0$ is the wavenumber with the sound speed c_0 enclosed between two flat interface.

Denote u to be the scattering field. The solution of the acoustic scattering problem by the scatterer D in an oceanic waveguide R_H^2, is to find a function u such that it satisfies the following equations:

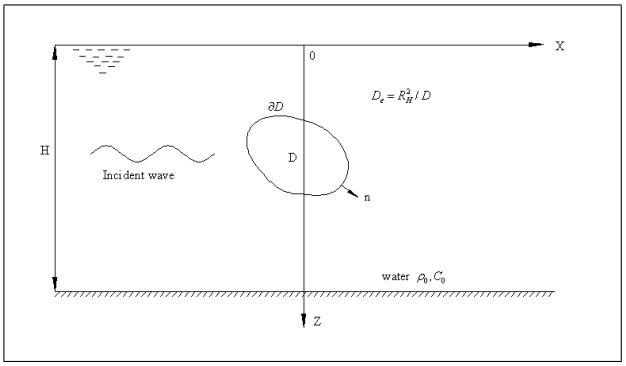

Figure 1. Sketch of the problem.

$$\begin{cases} \Delta u + k^2 u = 0, & \text{in } D_e, \\ u = -u^i, & \text{on } \partial D, \\ \dfrac{\partial u}{\partial z}\Big|_{z=H} = 0, \quad u\big|_{z=0} = 0. \end{cases} \quad (2)$$

Note that the scattering field u has the modal representation for $(x, z) \in R_H^2$

$$u = \sum_{n=0}^{+\infty} \phi_n(z)\, u_n(x), \quad (3)$$

where the nth mode u_n of u must be satisfied the generated radiation condition

$$\lim_{r\to+\infty} r^{1/2}\Big(\frac{\partial u_n}{\partial r} - \mathrm{i}k_n u_n\Big) = 0, \ n = 1, 2, \cdots, \ r = |x|. \quad (4)$$

3. The coupled FE and DtN mapping method

The standard approach of solving the Helmholtz equation using finite elements is based on Galerkin method. In order to implement such a Galerkin method, one must first transfer the unbound domain into a bound domain,i.e., an artificial boundaryΓ need to be introduced such that the original infinite domain in $R^m (m = 2, 3)$ is divided into two domains: a finite computational domain Ω and an infinite residual domain $R^m \backslash \Omega$. Then, one may first solve the problem analytically in $R^m \backslash \Omega$, and hence use the solution to find the Dirichlet-to-Neumann mapping(i.e. the DtN mapping) on the artificial boundary Γ. Finally, the DtN mapping is used as a boundary condition on Γ to obtain a well-posed problem in Ω, and hence the problem in Ω is solved numerically by the finite-element method (i.e. FEM). We call the above procedure as a coupled FE and DtN mapping method.

To do so, we partition the water layer exterior to D into three subdomains:

$$\Omega_1 = \big\{(x, z) \in D_e \big| x \le -R_1\big\},$$
$$\Omega_2 = \big\{(x, z) \in D_e \big| -R_1 \le x \le R_2\big\},$$
$$\Omega_3 = \big\{(x, z) \in D_e \big| x \ge R_2\big\},$$

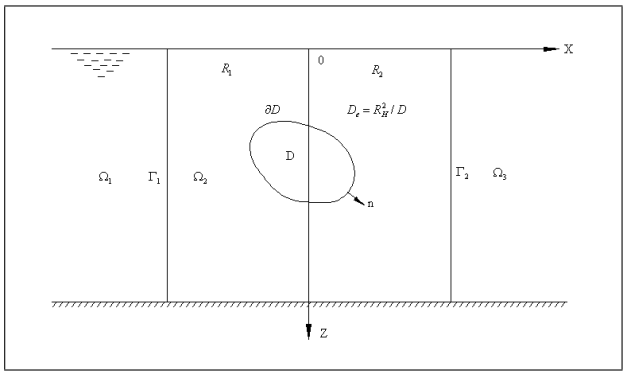

Figure 2. Sketch of The Coupled FE and DtN Mapping Method

and denote the common boundaries between the subdomains Ω_1 and Ω_2, Ω_2 and Ω_3 by $\Gamma_1 = \{(x,z)|x = -R_1, 0 \le z \le H\}$ and $\Gamma_2 = \{(x,z)|x = R_2, 0 \le z \le H\}$ respectively, as shown in Figure 2.

Then the exterior problem (2) of the Helmholtz equation in a shallow water can now be transformed into the following interior problem. That is, for$(x,z) \in \Omega_2$, to find a function u such that it satisfies the following equations:

$$\begin{cases} \Delta u + k^2 u = 0, & \text{in } \Omega_2, \\ \dfrac{\partial u}{\partial z}\Big|_{z=H} = 0, \quad u\Big|_{z=0} = 0, \\ u = -u^i, & \text{on } \partial D, \\ \dfrac{\partial u}{\partial \mathbf{n}} = M_1(u), & \text{on } \Gamma_1, \\ \dfrac{\partial u}{\partial \mathbf{n}} = M_2(u), & \text{on } \Gamma_2, \end{cases} \tag{5}$$

where $\mathbf{n}$ is the outward unit normal to Γ_1 and Γ_2, M_1 and M_2 are the DtN mapping on the artificial boundaries Γ_1 and Γ_2.

In order to solve the interior problem (5), the DtN mapping M_1 and M_2 must first be obrained. To this end, by use of the eigenfunction expansion method, the scattering fields $u_1$and u_3 in the exterior subdomains Ω_1 and Ω_3 can be represented respectively as following:

$$u_1(x,z) = \sum_{n=1}^{+\infty} u_{1n}\,\phi_n(z)\,\mathrm{e}^{-\mathrm{i}k_n(x+R_1)}, \quad x \le -R_1, \tag{6}$$

$$u_3(x,z) = \sum_{n=1}^{+\infty} u_{3n}\,\phi_n(z)\,\mathrm{e}^{\mathrm{i}k_n(x-R_2)}, \quad x \ge R_2. \tag{7}$$

From the orthogonal characteristics of the eigenfunction system $\{\phi_n(z)\}_{n=1}^{+\infty}$ in $[0, H]$, we can obtain

$$u_1(x,z) = \sum_{n=1}^{+\infty} \phi_n(z)\,\mathrm{e}^{-\mathrm{i}k_n(x+R_1)} \cdot \int_0^H \phi_n(z)\,u_1(-R_1,z)\,\mathrm{d}z, \quad x \le -R_1, \tag{8}$$

$$u_3(x,z) = \sum_{n=1}^{+\infty} \phi_n(z)\,\mathrm{e}^{\mathrm{i}k_n(x-R_2)} \cdot \int_0^H \phi_n(z)\,u_3(R_2,z)\,\mathrm{d}z, \quad x \ge R_2, \tag{9}$$

and hence, the normal derivatives of the scattering fields u_1 and u_3 on Γ_1 and Γ_2 can be written as

$$\frac{\partial u_1(x,z)}{\partial x}\Big|_{x=-R_1} = -\mathrm{i}\sum_{n=1}^{+\infty} k_n\,\phi_n(z)\int_0^H \phi_n(z)u_1(-R_1,z)\,\mathrm{d}z, \tag{10}$$

$$\frac{\partial u_3(x,z)}{\partial x}\Big|_{x=R_2} = \mathrm{i}\sum_{n=1}^{+\infty} k_n\,\phi_n(z)\int_0^H \phi_n(z)\,u_3(R_2,z)\,\mathrm{d}z. \tag{11}$$

Note that the scattering fields must satisfy the continuity conditions on the artificial boundaries Γ_1 and Γ_2

$$u = u_1, \quad u_x = u_{1x}, \quad \text{on } \Gamma_1, \tag{12}$$

$$u = u_3, \quad u_x = u_{3x}, \quad \text{on } \Gamma_2. \tag{13}$$

Combining (8)—(13), we obtain

$$\begin{aligned} M_1(u) &= -\frac{\partial u(x,z)}{\partial x}|_{x=-R_1} \\ &= \mathrm{i}\sum_{n=1}^{+\infty} k_n\,\phi_n(z)\int_0^H \phi_n(z)\,u(-R_1,z)\,\mathrm{d}z, \end{aligned} \tag{14}$$

$$\begin{aligned} M_2(u) &= \frac{\partial u(x,z)}{\partial x}|_{x=R_2} \\ &= \mathrm{i}\sum_{n=1}^{+\infty} k_n\,\phi_n(z)\int_0^H \phi_n(z)\,u(R_2,z)\,\mathrm{d}z. \end{aligned} \tag{15}$$

Then we can now start with the solution of the interior problem (5) based on the Galerkin method. To this end, we define the tried function space as following:

$$U = \left\{u \,\middle|\, u \in H^1(\Omega_2),\ u\Big|_{z=0} = 0,\ u\Big|_{\Gamma} = -u^i\right\}, \tag{16}$$

$$W = \left\{w \,\middle|\, w \in H^1(\Omega_2),\ w\Big|_{z=0} = 0,\ w\Big|_{\Gamma} = 0\right\}, \tag{17}$$

where$H^1(\Omega_2)$ is the Sobolev space on the subdomain Ω_2 .

Now, the statement of the equivalent form of the interior problem (5) is: Find a function $u \in U$ such that for any $w \in W$

$$a(u,w) - b(u,w) = 0, \tag{18}$$

where

$$a(u,w) = \int_{\Omega_2} \nabla u \cdot \nabla \bar{w}\,\mathrm{d}\Omega - k^2 \int_{\Omega_2} u\bar{w}\,\mathrm{d}\Omega, \tag{19}$$

$$b(u,w) = \int_{\Gamma_1} M_1(u)\bar{w}\,\mathrm{d}s + \int_{\Gamma_2} M_2(u)\bar{w}\,\mathrm{d}s. \tag{20}$$

In the following section, we will present the numerical approach of the Galerkin approximation problem(21).

4. Numerical method

In order to numerically solve the Galerkin problem (18), we partition the subdomain Ω_2 into some finite elements. Let $\{\psi_j\}|_{j=1}^{Nel}$ be the set of local interpolation basis functions, where Nel is the total number. Denote U_h and W_h to be linear function space spanned by $\{\psi_j\}|_{j=1}^{Nel}$. Then, the Galerkin approximation to the interior problem (5)

is obtained by considering the finite-dimensional spaces $U_h \subset U$ and $W_h \subset W$, and then seeking an approximate solution to (5): Find a function $u_h \in U_h$ such that for any $w_h \in W_h$

$$a(u_h, w_h) - b(u_h, w_h) = 0. \tag{21}$$

For $(x, z) \in \Omega_2$, we have

$$\begin{aligned} u_h(x, z) &= \sum\nolimits_{l=1}^{Nel} u_l \psi_l(x, z), w_h(x, z) \\ &= \sum\nolimits_{l=1}^{Nel} w_l \psi_l(x, z), \end{aligned} \tag{22}$$

where u_l and w_l are the values of the functions u and w on the lth node respectively.

Substitute (22) into (19), then we have

$$a(u_h, w_h) = \sum_{l=1}^{Nel}\sum_{j=1}^{Nel} \bar{w}_l \left[\int_\Omega \left\{\nabla\bar{\psi}_l \nabla\psi_j - k^2 \psi_l \psi_j\right\} \mathrm{d}\Omega\right] u_j. \tag{23}$$

With $\hat{U}_h = [u_1, u_2, \cdots, u_{Nel}]^T$, $\hat{W}_h = [w_1, w_2, \cdots, w_{Nel}]^T$, equation (23) can be represented as

$$a(u_h, w_h) = \overline{\hat{W}_h}\, K_a\, \hat{U}_h^T, \tag{24}$$

where $\hat{U}_h^T$ is the transpose matrix of $\hat{U}_h$ and K_a is the total stiffness matrix.

Note that the numerical computation of the second term in (21) involves the evaluation of the integrals on the artificial boundary Γ_1 and Γ_2 in (20). Therefore, the interpolation basis functions on the artificial boundary Γ_1 and Γ_2 must be constructed. To this end, let us denote $z_0^{(n)}, z_1^{(n)}, z_2^{(n)}, \cdots, z_{p^{(n)}}^{(n)}$ be the vertical coordinates of the nodes on the artificial boundary $\Gamma_n (n = 1, 2)$. Then, the interpolation basis function on the artificial boundary Γ_n can be given by

$$\varphi_j^{(n)} = \begin{cases} (z - z_{j-1}^{(n)})/h_j^{(n)}, & z_{j-1}^{(n)} \le z \le z_j^{(n)}, \\ (z_{j+1}^{(n)} - z)/h_{j+1}^{(n)}, & z_j^{(n)} \le z \le z_{j+1}^{(n)}, \\ & 1 \le j \le p^{(n)} - 1, \\ 0, & \text{others} \end{cases} \tag{25}$$

$$\varphi_0^{(n)} = \begin{cases} (z_1^{(n)} - z)/h_1^{(n)}, & z_0^{(n)} \le z \le z_1^{(n)}, \\ 0, & \text{others} \end{cases} \tag{26}$$

$$\varphi_p^{(n)} = \begin{cases} (z - z_{p^{(n)}-1}^{(n)})/h_p^{(n)}, & z_{p^{(n)}-1}^{(n)} \le z \le z_{p^{(n)}}^{(n)}, \\ 0, & \text{others}, \end{cases} \tag{27}$$

where $p^{(n)}$ is the nodal number on the artificial boundary Γ_n, $h_j^{(n)} = (z_j^{(n)} - z_{j-1}^{(n)})/p^{(n)}$, $j = 1, 2, \cdots, p^{(n)}$.

Based on the interpolation basis function defined above, then for $(x, z) \in \Gamma_1$ or Γ_2, we have

$$\begin{aligned} u_h(-R_1, z) &= \sum\nolimits_{j=0}^{p^{(1)}} u_{L_1(j)}\, \varphi_j^{(1)}, \\ u_h(R_2, z) &= \sum\nolimits_{j=0}^{p^{(2)}} u_{L_1(j)}\, \varphi_j^{(2)} \\ w_h(-R_1, z) &= \sum\nolimits_{j=0}^{p^{(1)}} w_{L_1(j)}\, \varphi_j^{(1)}, \\ w_h(R_2, z) &= \sum\nolimits_{j=0}^{p^{(2)}} w_{L_1(j)}\, \varphi_j^{(2)}, \end{aligned} \tag{28, 29}$$

where $L_n(j)$ is the total nodal number at the point $z = z_j^{(n)}$ on Γ_n.

Substituting (28) and (29) into (20), we have

$$\begin{aligned} &\int_{\Gamma_1} M_1(u_h)\bar{w}_h \,\mathrm{d}s = \\ &\mathrm{i}\sum_{n=1}^{+\infty} k_n \int_0^H \phi_n(z)\bar{w}_h(-R_1, z)\,\mathrm{d}z \int_0^H \phi_n(z) u_h(-R_1, z)\,\mathrm{d}z \\ &= \sum_{n=1}^{+\infty} k_n \left\{ \sum_{l=0}^{p^{(1)}} \bar{w}_{L_1(l)} \left[\int_0^H \phi_n(z)\varphi_l^{(1)}(z)\,\mathrm{d}z\right] \right. \\ &\qquad \left. \cdot \sum_{j=0}^{p^{(1)}} \left[\int_0^H \phi_n(z)\varphi_j^{(1)}(z)\,\mathrm{d}z\right] u_{L_1(j)} \right\}, \end{aligned} \tag{30}$$

$$\begin{aligned} &\int_{\Gamma_2} M_2(u_h)\bar{w}_h \,\mathrm{d}s = \\ &\mathrm{i}\sum_{n=1}^{+\infty} k_n \int_0^H \phi_n(z)\bar{w}_h(R_2, z)\,\mathrm{d}z \int_0^H \phi_n(z) u_h(R_2, z)\,\mathrm{d}z \\ &= \sum_{n=1}^{+\infty} k_n \left\{ \sum_{l=0}^{p^{(2)}} \bar{w}_{L_2(l)} \left[\int_0^H \phi_n(z)\varphi_l^{(2)}(z)\,\mathrm{d}z\right] \right. \\ &\qquad \left. \cdot \sum_{j=0}^{p^{(2)}} \left[\int_0^H \phi_n(z)\varphi_j^{(2)}(z)\,\mathrm{d}z\right] u_{L_2(j)} \right\}. \end{aligned} \tag{31}$$

We now define the following matrix K_L and K_R follows:

$$K_L\big(L_1(l), L_1(j)\big) = \sum_{n=1}^{+\infty} k_n \left\{ \sum_{l=0}^{p^{(1)}} \int_0^H \phi_n(z)\varphi_l^{(1)}(z)\,\mathrm{d}z \sum_{j=0}^{p^{(1)}} \int_0^H \phi_n(z)\varphi_j^{(1)}(z)\,\mathrm{d}z \right\}, \tag{32}$$

$$K_R\big(L_2(l), L_2(j)\big) = \sum_{n=1}^{+\infty} k_n \left\{ \sum_{l=0}^{p^{(2)}} \int_0^H \phi_n(z)\varphi_l^{(2)}(z)\,\mathrm{d}z \sum_{j=0}^{p^{(2)}} \int_0^H \phi_n(z)\varphi_j^{(2)}(z)\,\mathrm{d}z \right\}, \tag{33}$$

Then, we have

$$b(u_h, w_h) = \overline{\hat{W}_h}(K_L + K_R)\hat{U}_h^T. \tag{34}$$

Combining (24) and (34), the Galerkin approximation problem(21) can rewrriten as

$$\overline{\hat{W}_h}(K_a - K_L - K_R)\hat{U}_h^T = 0. \tag{35}$$

Due to the arbitrariness of $\hat{W}_h$, we have

$$K\hat{U}_h^T = 0, \tag{36}$$

where $K = K_a - K_L - K_R$.

This is the finite-element stiffness equation for numerically solving Galerkin approximation problem (21). We see that the effect of the DtN boundary condition on the above finite element scheme is included in the stiffness matrix K. Note that K_L and K_R are nonzero only if the nodes lie on the artificial boundaries Γ_1 and Γ_2.

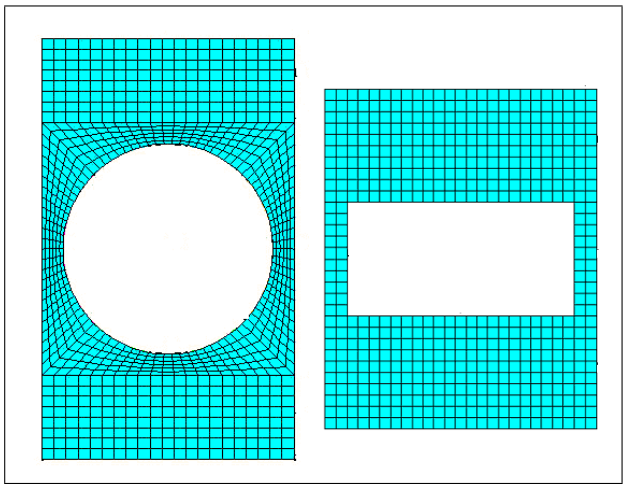

Figure 3. The partitions for an infinite long circular and rectangle cylinder.

5. Numerical results

Let L be the characteristic length of the scattering object. The two classes of such scattering objects are considered as following:

1. The infinite long rectangular cylinder with the width L and the height $L/2$.
2. The infinite long circular cylinder with the diameter L.

The isoparametric elements with 4 nodes are used for the subdomain Ω_2, where the 94 equidistant points are taken for the partition of the boundary of the scattering object, the 23 equidistant points are taken for the partitions of the free surface and the rigid bottom, and the 20 equidistant points are taken for the partitions of the artificial boundaries Γ_1 and Γ_2. The result is shown in figure 3. Furthur, the integrals in (23) are computed by use of the Guass integral method with 5 nodes, and the integrals in (33) and (34) can be computed analytically. Except for the special explanation, the center of the scattering object is taken to be$(0, H/2)$, and for the determination of the artificial boundary Γ_1 and Γ_2, we take $R_1 = R_2 = R$. Finally, the infinite series in (33) and (34) are taken to be the front 1000 terms.

To exam the validity of the coupled FE and DtN mapping method, we first consider the case where the incident source point $(x_s, z_s)$is located at the center of the scattering objects. In this case, the scattering field u has the exact solution $u_{exact} = -u^i$. Denote Λ to be the set of all nodes and define the maxim nodal error to be

$$Er = \max_{(x,z)\in\Lambda} \left\{ \frac{\left| u_h(x,z) - u_{exact}(x,z) \right|}{\left| u_{exact}(x,z) \right|} \right\}. \qquad (37)$$

In the following computations, the water depth is taken as $H = 1.5L, 3.5L$ and $5.5L$ for infinite long rectangle cylinder, and $H = 2L, 3L$ and $4L$ for infinite long circular cylinder. Results are showed in figures 4 and 5. It can be found from these figures that the computational results based the proposed method are in good agreements with the ones based on the exact solution. Therefore, the proposed method is reasonable and valid.

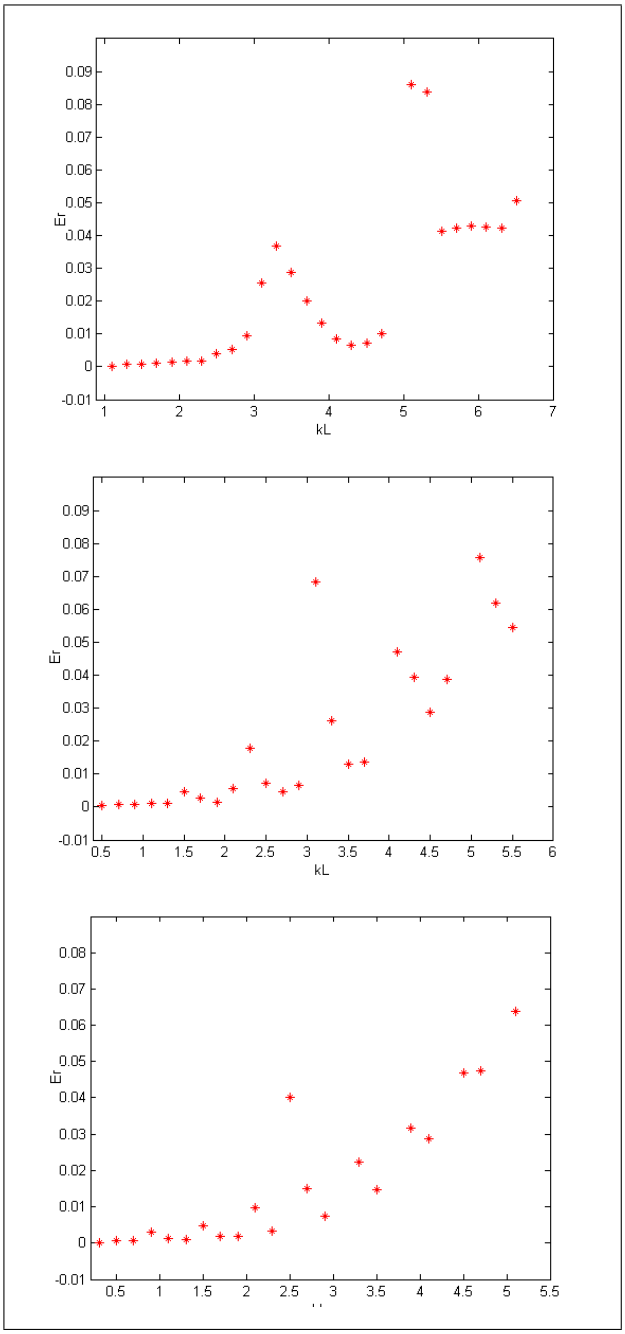

Figure 4. The maxim nodal errors between the proposed method and the exact solution for an infinite long rectangle cylinder with the center $(0, H/2)$ where the incident line source is located at $(0, H/2)$, the depth of the ocean is $H = 1.5L$, $H = 3.5L$ and $H = 5.5L$ from the left to the right respectively.

From the Figures 4 and 5, we can further find that the proposed method is much ideal for the case of frequency in the resonance range. However, it needs to be pointed out that the accuracy of the solutions by the proposed method deteriorates rapidly with increasing non-dimensional wavenumber, even when the number of elements per wavelength is kept constant. This error is mainly originated from the numerical dissipation between

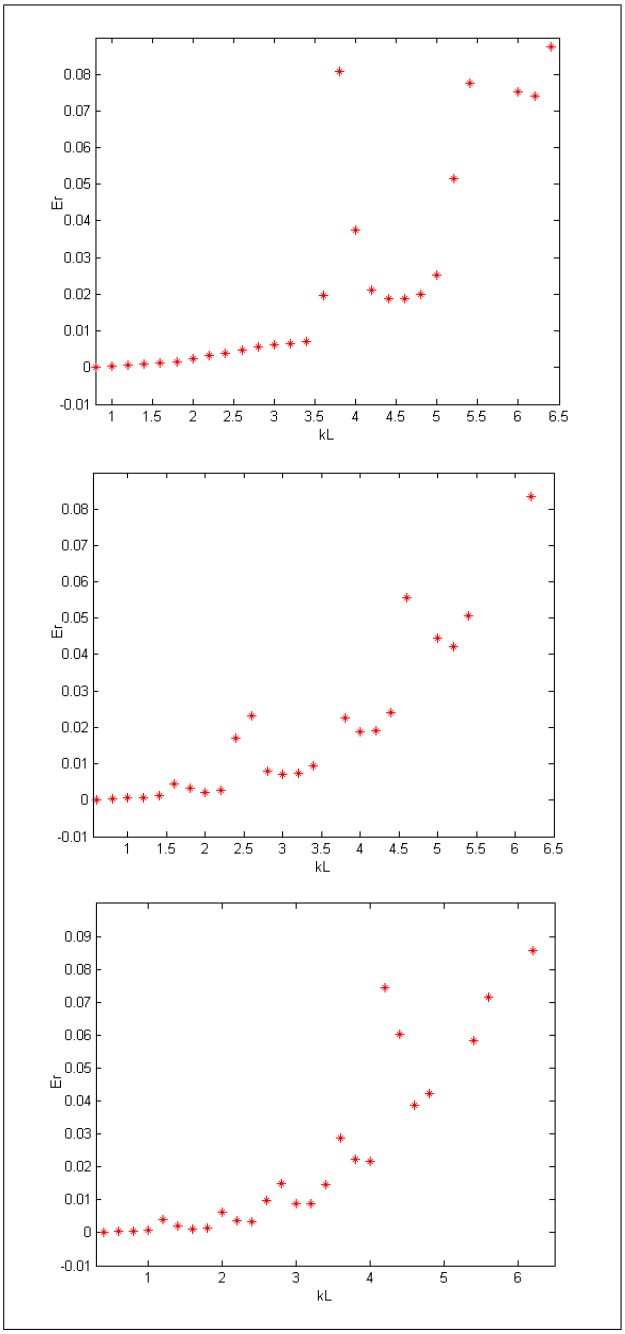

Figure 5. The maxim nodal errors between the proposed method and the exact solution for an infinite long circular cylinder with the center $(0, H/2)$ where the incident line source is located at $(0, H/2)$, the depth of the ocean is $H = 2L$, $H = 3L$ and $H = 4L$ from the left to the right respectively.

the continuous and numerical wavenubers induced by the Galerkin method[3]. There are some methods to quantify the pollution error for the case of the free space [21], [22]. However, how to overcome the pollution error for the case of the oceanic waveguide will be further studied in the future work.

We would also like to point out that the computational efficiency is very high even when the nodal numbers are high because of the sparseness of the finite-element stiffness matrix. For the present examples, it only needs 333 seconds or so in the Dell computer workstation with the 3.0GHz CPU when the nodal numbers are over $Nel = 9665$.

In the following examples, we consider the influence of the multiple scattering effects between the free surface and the rigid bottom on the propagation characteristics of the scattering field by a scattering object when the incident line source lies at the exterior of the scattering object.

We first consider the case where the water depth is taken as $H = 3.5L$, the non-dimensional wavenumber is taken as $kL = 2$, the incident line sources are located at $(-100L, 0.25H)$, $(-100L, 0.5H)$ and $(-100L, 0.75H)$, and the scattering object is taken as the infinite long rectangle cylinder. The results are shown in figures 6 and 7. It follows from these figures that the multiple scattering effects of the free surface or the bottom are dominant when the incident line source is near the free surface or the bottom. However, the multiple scattering effects of the free surface or the bottom are smaller when the incident line source is far from the free surface or the bottom.

We further consider the case where the non-dimensional wavenumber is taken as $kL = 2$, the incident line source is located at $(-100L, 0.5H)$, the scattering object is taken as the infinite long circular cylinder centered at $(0, L)$, $(0, 2L)$ and $(0, 3L)$. The results are shown in figures 8 and 9. It follows from these figures that the multiple scattering effects are strong when the scattering object is nearer the free surface or the bottom, but weak when the scattering object is far from the free surface or the bottom.

6. Conclusions

A coupled FE and DtN mapping method is proposed for the acoustic scattering problem by a scattering object in an oceanic waveguide, which is achieved by the solutions of the Helmholtz equation in two exterior and an interior domains. The solutions of Helmholtz equation in two exterior domains are analytically expressed by use of the eigenfunction expansion method. The DtN mapping is obtained to define the solution of the Helmholtz equation in a interior domain, and then a finite element method based on the Galerkin variational principle is presented for the numerical solution of the Helmholtz equation in the interior domain.

Based on the proposed method, the numerical simulation and analysis of the acoustic scattering problem for an infinite long rectangle and circular cylinders are performed. The numerical results show that the computational results based on the proposed method is in good agreement with the ones based on exact solution for frequency in resonant range, and hence indicate the validity and practicality of the proposed method. The results further show that the multiple scattering effects between the free surface and the bottom have remarkably influence on the propagation characteristics of the scattering field by a scattering object in the oceanic waveguide.

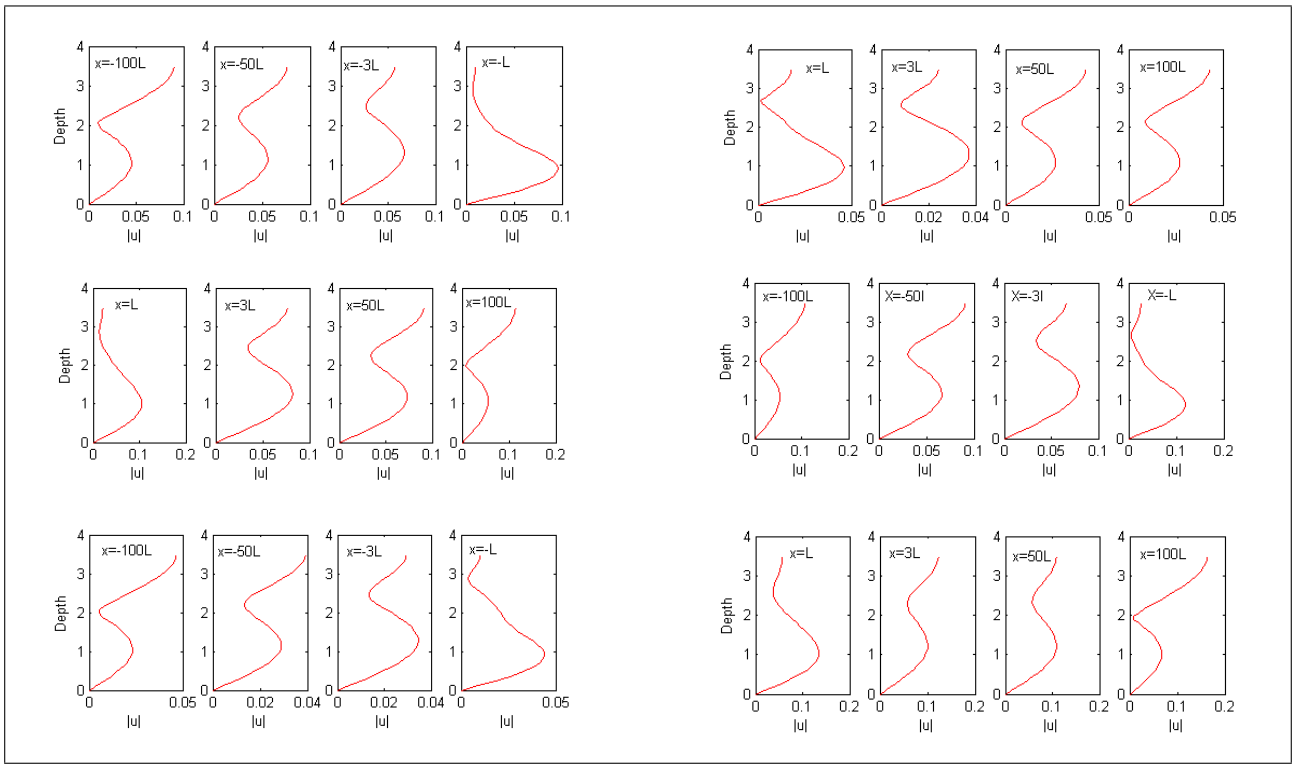

Figure 6. The scattered fields on the vertical sections $x = \pm L$, $\pm 3L$, $\pm 50L$ and $\pm 100L$ for an infinite long rectangle cylinder with the center$(0, H/2)$ when the water depth $H = 3.5L$, the non-dimensional wavenumber $kL = 2$, the incident line sources are located at $(-100L, 0.25H)$(up), $(-100L, 0.5H)$(middle) and $(-100L, 0.75H)$(down) respectively.

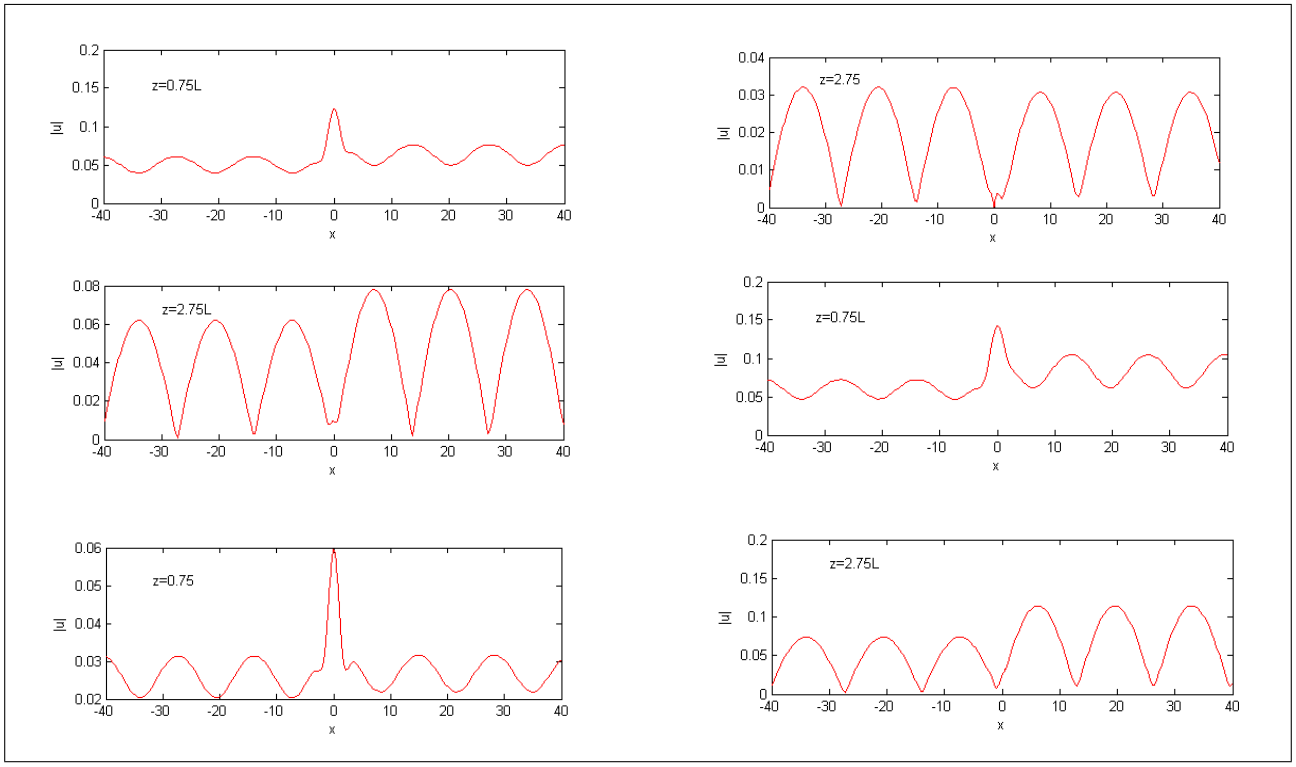

Figure 7. The scattered fields on the horizontal sections $z = 0.75L$ and $z = 2.75L$ for an infinite long rectangle cylinder with the center $(0, H/2)$ when the water depth $H = 3.5L$, the non-dimensional wavenumber $kL = 2$, the incident line sources are located at $(-100L, 0.25H)$(up), $(-100L, 0.5H)$ (middle) and $(-100L, 0.75H)$(down) respectively.

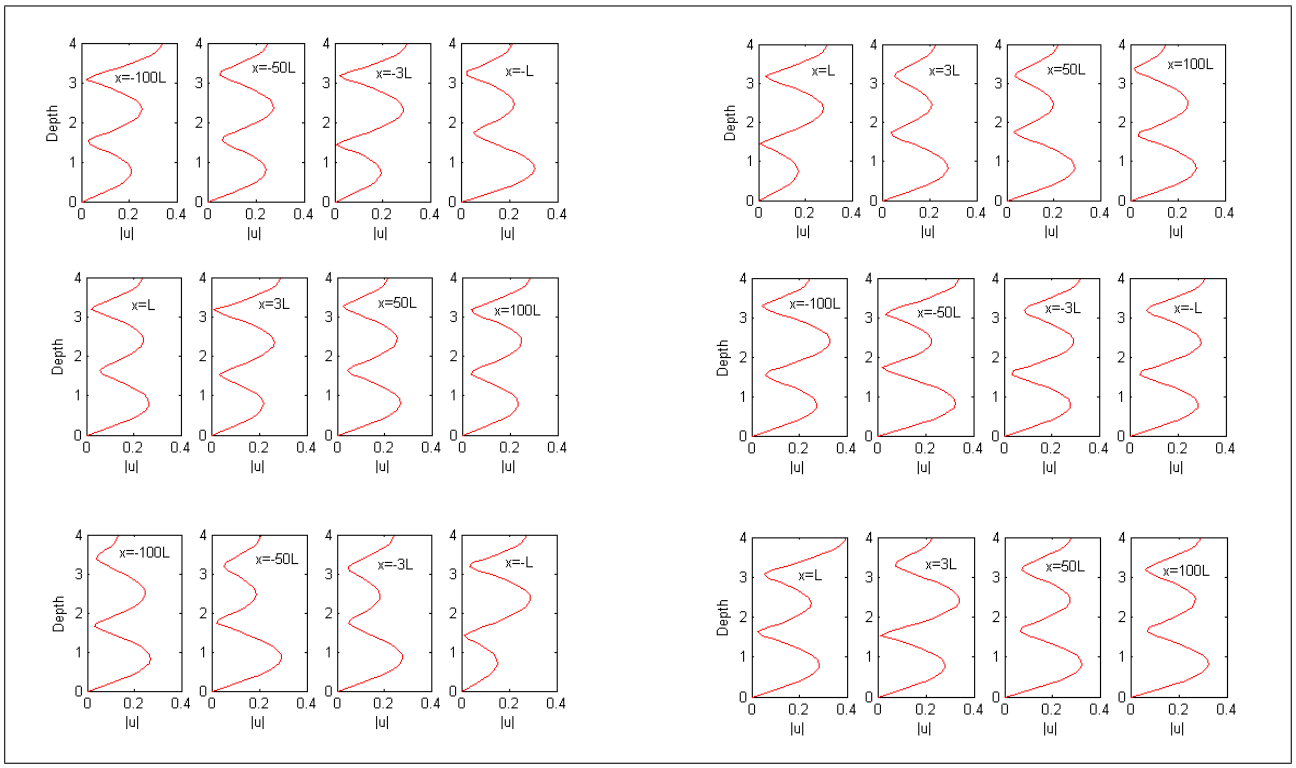

Figure 8. The scattered fields on the vertical sections $x = \pm L, \pm 3L, \pm 50L$ and $\pm 100L$ for an infinite long circular cylinder when the water depth $H = 4L$, the non-dimensional wavenumber $kL = 2$, the incident line source is located at $(-100L, 0.5H)$, the centers of the scattering object are located at $(0, L)$(up),$(0, 2L)$(middle) and $(0, 3L)$ (down) respectively.

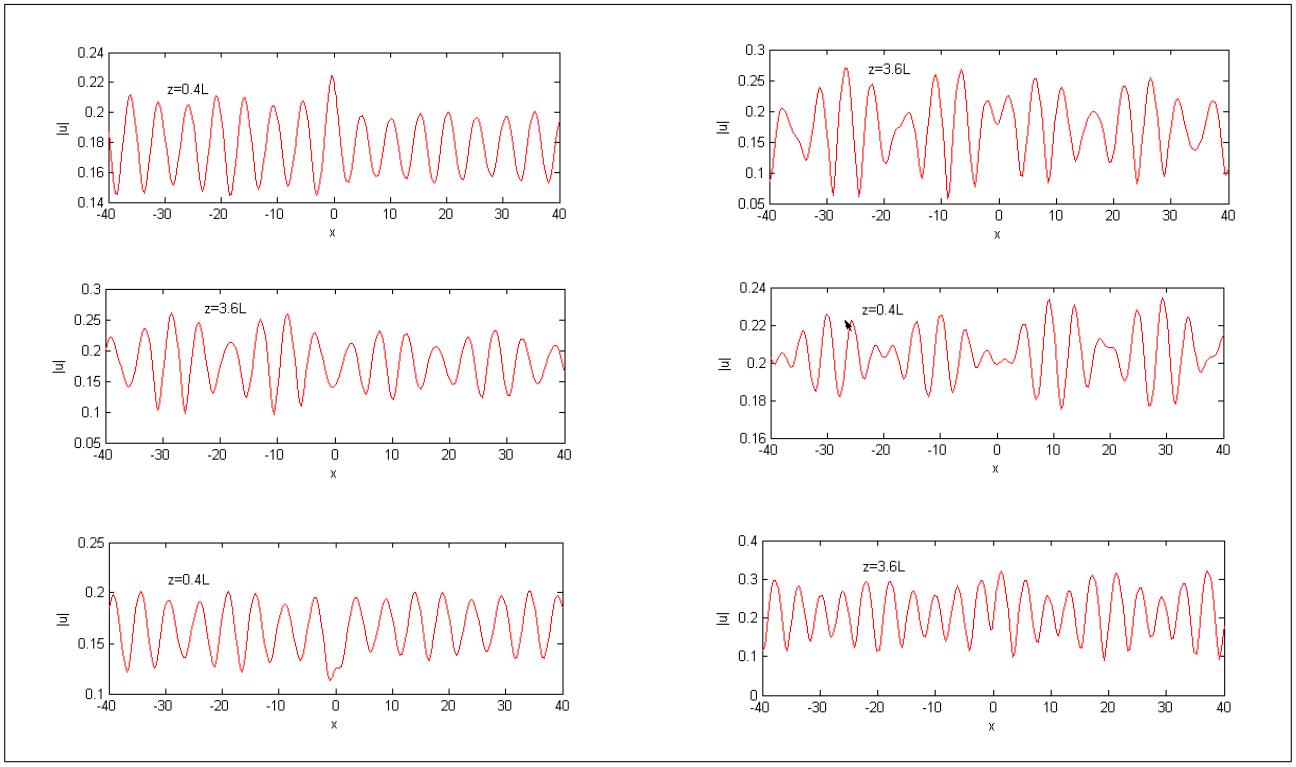

Figure 9. The scattered fields on the horizontal sections $z = 0.4L$ and $z = 3.6L$ for an infinite long circular cylinder when the water depth $H = 4L$, the non-dimensional wavenumber $kL = 2$, the incident line source is located at $(-100L, 0.5H)$, the centers of the scattering object are located at $(0, L)$(up),$(0, 2L)$(middle) and $(0, 3L)$(down) respectively.

Acknowledgement

The authors would like to thank the referees for their helpful suggestion. This work was partially supported by the National Nature Science Foundation of China under Grant No. 10672128, and partially by the Doctor Foundation (471-38650238) and the Undergraduate Innovative Foundation (A145) of Wuhan University of Technology.

References

[1] C. A. Brebbia, J. F. C. Telles, L. C. Wrobel: Boundary element techniques. Springer Verlag, Berlin, 1984.

[2] A. J. Burton, G. F. Miller: The application of integral equation methods to the numerical solution of some exterior boundary-value problems. Proc. Royal Soc. London **323** (1971) 201–220.

[3] F. Ihlenburg: Finite element scattering of acoustic scattering. 1stedition. Springer Verlag, New York, 1998.

[4] J. A. Fawcett, T. W. Dawson: Fourier synthesis of three-dimensional scattering in an oceanic waveguide using two-dimensional boundary integral equation methods. J. Acoustic. Soc. Am. **88** (1990) 1913–1920.

[5] T. W. Dawson: Acoustic scattering in a three-dimensional oceanic waveguide using two-dimensional boundary integral equation methods. J. Acoustic. Soc. Am. **90** (1991) 2609–2621.

[6] Y. Z. Xu, Y. Yan: An approximate boundary integral method for acoustic scattering in shallow oceans. J. Comput. Acoust. **1** (1993) 61–75.

[7] J. A. Fawcett: An effective three-dimensional boundary integral equation method for solving azimuthally symmetric scattering problems in the oceanic waveguide. J. Acoustic. Soc. Am. **94** (1993) 2307–2314.

[8] T. W. Wu: On computational aspects of the boundary element method acoustic radiation and scattering in a perfect waveguide. J. Acoustic. Soc. Am. **96** (1994) 3733–3743.

[9] I-Tai, Lu: Analysis of acoustic wave scattering by scatterers in layered media using the hybrid ray-mode (boundary integral equation) method. J. Acoustic. Soc. Am. **86** (1989) 1136–1142.

[10] M. Fischer, U. Gauger, L. Gaul: A multipole galerkin boundary element method for acoustics. Engineering Analysis with Boundary Elements **28** (2004) 155–162.

[11] M. Fischer, L. Gaul: Application of the fast multipole BEM for structural-acoustic simulations. Journal of Computational Acoustics **13** (2005) 87–98.

[12] S. Marburg, S. Schneider: Performance of iterative solvers for acoustic problems. Part I: Solvers and effect of diagonal preconditioning. Engineering Analysis with Boundary Elements **27** (2003) 727–750.

[13] T. Sakuma, Y. Yasuda: Fast multipole boundary element method for large-scale steady-state sound field analysis, Part I: Setup and validation. Acustica united with Acta Acustica **88** (2002) 513–525.

[14] T. Sakuma, Y. Sakuma: Fast multipole boundary element method for large-scale steady-state sound field analysis, Part II: Examination of numerical items. Acustica united with Acta Acustica **89** (2003) 28–38.

[15] S. Schneider: Application of fast methods for acoustic scattering and radiation problems. Journal of Computational Acoustics **11** (2003) 387–401.

[16] S. Marburg, S. Amini: Cat's eye radiation with boundary elements: Comparative study on treatment of irregular frequencies. Journal of Computational Acoustics **13** (2005) 21–45.

[17] F. Kang: Asymptotic radiation conditions for reduced wave equation. J. Comput. Math. **2** (1984) 130–138.

[18] D. Givoli: Recent advances in the DtN and FE method. Archives of Computational Methods in Engineering **6** (1999) 71–116.

[19] I. Harari: A survey of finite element methods for time-harmonic acoustics. Computer Methods in Applied Mechanical Engineering **195** (2006) 1594–1607.

[20] L. L. Thompson: A review of finite element methods for time-harmonic acoustics. Journal of the Acoustical Society of America **119** (2006) 1315–1330.

[21] A. A. Oberai, P. M. Pinsky: A residual-based finite element method for the Helmholtz equation. Int. J. Numer. Meth. Engng. **49** (2000) 399–419.

[22] O. Cessenat, B. Despres: Appication of an ultra weak variational formulation of elliptic pdes to the two-dimensional Helmholtz equation. SIAM J. Numer. Anal. **35** (1998) 255–299.